

## INVESTIGATION OF $^{41}\text{Sc}$ BY PROTON CAPTURE IN $^{40}\text{Ca}$

F. ZIJDERHAND, R.C. MAKKUS and C. VAN DER LEUN

*Fysisch Laboratorium, Rijksuniversiteit Utrecht, PO Box 80.000, 3508 TA Utrecht, The Netherlands*

Received 20 November 1986

**Abstract:** Resonance strengths, excitation energies and  $\gamma$ -ray branching ratios have been measured of twenty  $^{40}\text{Ca}(p, \gamma)^{41}\text{Sc}$  resonances observed in the  $E_p = 640\text{--}3500$  keV region. The reaction  $Q$ -value is determined as  $Q = 1085.07 \pm 0.09$  keV. A previously not reported  $^{41}\text{Sc}$  level is found at  $E_x = 3.01$  MeV; it is the missing mirror state of  $^{41}\text{Ca}$  (3.05 MeV).

Gamma-ray angular distributions, measured at three selected resonances, lead to the assignments  $J^\pi = \frac{3}{2}^+, \frac{7}{2}^+$  and  $\frac{7}{2}^-$  to the  $E_x = 2.10, 3.70$  and  $4.03$  MeV levels, respectively. A spin  $J^\pi = \frac{3}{2}^-$  is assigned to the  $E_x = 2.41$  MeV level on the basis of transition strength arguments.

These new data allow a rather detailed comparison of the mirror states of  $^{41}\text{Ca}$  and  $^{41}\text{Sc}$ . Shell-model calculations are performed for the  $A = 38\text{--}42$  mass region, based on a  $(2s_{1/2}1d_{3/2})\text{--}(1f_{7/2}2p_{3/2})$  configuration space with up to three (four for  $A = 40$ ) particles excited from the  $sd$  to the  $fp$  shell. Both positive- and negative-parity states are considered. Excitation energies and transition strengths of  $A = 41, T = \frac{1}{2}$  nuclei are calculated and compared to the experimental data.

E

NUCLEAR REACTIONS  $^{40}\text{Ca}(p, \gamma)$ ,  $E = 640\text{--}3500$  keV; measured  $\sigma(E_p)$ ,  $\sigma(E_\gamma, \theta)$ ,  $\gamma$ -yield; deduced  $Q$ .  $^{41}\text{Sc}$  deduced levels,  $\gamma$ -branchings,  $J, \pi, \delta, \Gamma_\gamma, \Gamma_p, \Gamma$ . Compton-suppression spectrometer, natural target. Shell-model calculations.  
NUCLEAR STRUCTURE  $A = 38\text{--}42$ ; calculated levels,  $B(\lambda)$ .

### 1. Introduction

The mirror nuclei  $^{41}\text{Ca}$  and  $^{41}\text{Sc}$  are of interest both experimentally and theoretically, since both nuclei have only one nucleon bound to the doubly-magic  $^{40}\text{Ca}$  core. The level structure of these nuclei is, however, much more complicated than expected on the basis of simple shell-model considerations, because excitations of the  $^{40}\text{Ca}$  core by vibrational and/or many-particle-many-hole excitations play a significant role.

The reported experimental data <sup>1)</sup> on the  $^{41}\text{Sc}$  nucleus are remarkably scarce. The spins of several low-lying states are not yet determined and hardly any  $\gamma$ -ray transition strengths other than for ground-state transitions are known.

Proton capture by  $^{40}\text{Ca}$  is a very suitable reaction to investigate the nuclide  $^{41}\text{Sc}$ . A large fraction of the available data on  $^{41}\text{Sc}$  is due to  $^{40}\text{Ca}(p, p_0)^{40}\text{Ca}$  experiments <sup>2)</sup>. The  $^{40}\text{Ca}(p, \gamma)^{41}\text{Sc}$  reaction, however, has not yet been thoroughly investigated, mainly for technical reasons. Due to the low proton binding energy ( $Q = 1.09$  MeV) and the corresponding low energies of the decay  $\gamma$ -rays, the  $^{40}\text{Ca}(p, \gamma)^{41}\text{Sc}$  resonance cross sections are low. Since, moreover, all excited states of  $^{41}\text{Sc}$  are proton unbound, hardly any secondary  $\gamma$ -ray transitions can be observed. Finally, the detection of

the low-energy  $\gamma$ -rays from capture reactions is difficult due to the relatively high background.

The most extensive  $^{40}\text{Ca}(p, \gamma)^{41}\text{Sc}$  data reported so far are those of Youngblood *et al.*<sup>3)</sup> who measured the residual  $^{41}\text{Sc}(\beta^+)$  activity of the  $^{40}\text{Ca}(p, \gamma)^{41}\text{Sc}$  reaction in the range  $E_p = 0.6\text{--}5.2$  MeV and thus provide information about the ground-state decay of the  $^{40}\text{Ca}(p, \gamma)^{41}\text{Sc}$  resonances. The first experiment in which a Ge(Li) detector is used is the study by Kozub *et al.*<sup>4)</sup> of two  $^{40}\text{Ca}(p, \gamma)^{41}\text{Sc}$  resonances at  $E_p = 1843$  and  $5027$  keV. More recently Terrasi *et al.*<sup>5)</sup> investigated the  $^{40}\text{Ca}(p, \gamma)^{41}\text{Sc}$  direct capture reaction in the  $E_p = 2.1\text{--}3.1$  MeV range.

Due to the improved detection systems (Large-Angle Compton-Suppression Spectrometer with a large Ge detector, LACSS), accelerator performance and target handling (direct water-cooling) a more detailed investigation of the  $^{41}\text{Sc}$  nucleus via the  $^{40}\text{Ca}(p, \gamma)^{41}\text{Sc}$  reaction has now become feasible. In the present experiment the spins of several low-lying  $^{41}\text{Sc}$  levels and the  $\gamma$ -ray branching ratios of most  $^{41}\text{Sc}$  levels with  $E_x < 4.5$  MeV are determined.

This new information combined with literature data will be compared to the results of shell-model calculations. These calculations are performed for nuclei with masses  $A = 38\text{--}42$  in the  $(2s_{1/2}1d_{3/2})(1f_{7/2}2p_{3/2})$  configuration space with up to four particles excited from the *sd* to the *fp* shell. Even- and odd-parity states are considered in these calculations in which one set of six parameters describes the level structure of the nuclei in the mass region mentioned.

Sect. 2 of this paper describes the experimental set-up. The measurements of the yield curve are reported in sect. 3 and of the angular distributions in sect. 4. The shell-model calculations are presented in sect. 5, whereas sect. 6 summarizes and discusses the experimental and calculational results.

## 2. Experimental set-up

The proton beams for the present experiment are provided by the Utrecht 3 MV Van de Graaff accelerator. Beam currents up to  $150\ \mu\text{A}$  and proton energies up to  $E_p = 3.5$  MeV have been used. A  $90^\circ$  analyzing magnet combined with a corona feed-back system<sup>6)</sup> results in a proton energy resolution of better than  $200$  eV at  $E_p = 1850$  keV. The targets are produced by evaporating about  $40\ \mu\text{g}/\text{cm}^2$  natural calcium onto  $0.3$  mm thick tantalum backings, which are baked out before depositing the target material. This target thickness corresponds to an energy loss of about  $10$  keV for protons at  $E_p = 1850$  keV. Natural calcium has been chosen as target material, because it contains considerably less fluorine than the enriched  $^{40}\text{Ca}$ -metal or  $^{40}\text{CaCO}_3$  at our disposal. Even with the natural calcium targets, the high  $^{19}\text{F}(p, \alpha\gamma)^{16}\text{O}$   $\gamma$ -ray background is a problem. This background arises mainly from the fluorine in the calcium; the contribution of the fluorine in the backing is negligible. The directly water-cooled targets are replaced when the  $^{40}\text{Ca}(p, \gamma)$  yield is reduced by about  $30\%$ , i.e. after  $10$  to  $20$  h.

Two hyperpure germanium and two germanium–lithium detectors are used, all with an active volume of about 100 cm<sup>3</sup> and a resolution of 2.0 keV at  $E_\gamma = 1.33$  MeV. One germanium detector is used as part of a Compton-suppression spectrometer (LACSS) [ref. <sup>7</sup>], which reduced the Compton continuum by a factor of 10 to 20 (depending on  $E_\gamma$ ), whereas the loss at the full-energy peaks is negligible.

### 3. The <sup>40</sup>Ca(p, $\gamma$ )<sup>41</sup>Sc resonances

#### 3.1. YIELD CURVE MEASUREMENTS

The yield curve is measured over the  $E_p = 1500$ – $3200$  keV range in steps of 0.3–3 keV; at each point a complete  $\gamma$ -ray spectrum is measured and stored on magnetic tape. Since the resonances at lower energy ( $E_p < 2600$  keV) are very weak, the lower part of the yield curve has been measured with three  $\gamma$ -ray detectors; they are positioned at the angles  $\theta = +90^\circ$ ,  $0^\circ$  and  $-90^\circ$  relative to the proton-beam direction. For  $E_p > 2600$  keV only two  $\gamma$ -ray detectors have been used, positioned at  $\theta = +55^\circ$  and  $-55^\circ$ , which allowed a more straightforward determination of the resonance strengths.

Yield curves are produced off-line by setting various  $\gamma$ -ray energy windows. The  $\gamma$ -ray yield plotted in fig. 1 is the background-corrected content of a (sliding) narrow  $\gamma$ -ray energy window around the energy of the ground-state transition. Fig. 1 shows the raw data for the yield of one detector at  $\theta = 55^\circ$  (or scaled to represent this yield for  $E_p < 2600$  keV). The inserts show the yield of the  $r \rightarrow (1)$  transition at three resonances at which no ground-state transition could be observed. All resonances indicated in fig. 1 are due to the <sup>40</sup>Ca(p,  $\gamma$ )<sup>41</sup>Sc reaction and not to capture by other Ca isotopes or background elements. This is checked by comparing the measured proton and excitation energies (the latter as determined from the observed  $\gamma$ -ray energies which should be related according to  $E_x = Q + E_p M_{Ca} / (M_{Ca} + M_p)$ , with  $M_{Ca}$  and  $M_p$  the masses of the <sup>40</sup>Ca nucleus and of the proton, respectively. The detection limit for resonances in the measurement illustrated in fig. 1 corresponds to a ground-state transition resonance strength of about 5 meV. Several weaker resonances have nevertheless been studied in the present experiment (see sect. 3.2). Most of these states have been observed previously in the reactions <sup>40</sup>Ca(p, p<sub>0</sub>) [ref. <sup>2</sup>] and <sup>40</sup>Ca(p,  $\gamma$ )<sup>41</sup>Sc( $\beta^+$ )<sup>41</sup>Ca [ref. <sup>3</sup>]. The present experiment reveals one (p,  $\gamma$ ) resonance that has not been observed before; it is the  $E_p = 2540$  keV,  $E_x = 3563$  keV resonance, which most probably corresponds to the  $E_x = 3556 \pm 20$  keV level, previously observed in the <sup>41</sup>Ti( $\beta^+$ p) decay <sup>8</sup>).

The resonance strengths,  $S = (2J + 1)\Gamma_p\Gamma_\gamma/\Gamma$ , in which  $J$  denotes the resonance spin and  $\Gamma_p$ ,  $\Gamma_\gamma$  and  $\Gamma$  the proton, gamma-ray and total width, respectively, are determined from the yield-curve data. The strengths are measured relative to that of the <sup>40</sup>Ca(p,  $\gamma$ )<sup>41</sup>Sc resonance at  $E_p = 1843$  keV, for which  $S = 280 \pm 30$  meV has been reported <sup>9</sup>). A correction has been applied for target deterioration (below 10%

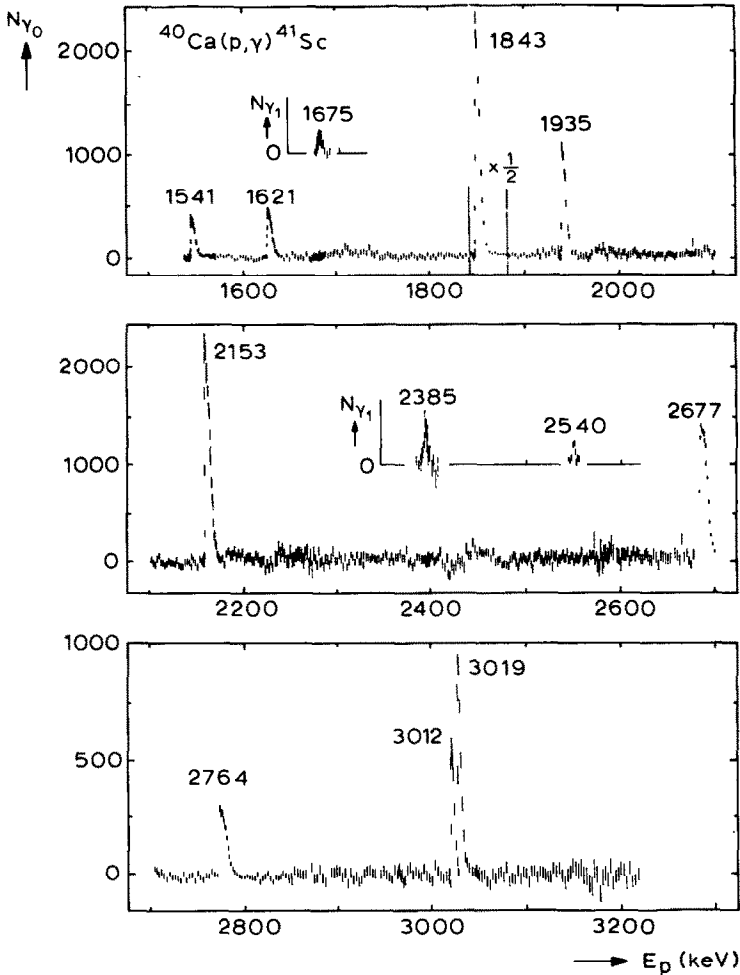


Fig. 1. Gamma-ray yield curve for the ground-state transition of the  $^{40}\text{Ca}(p, \gamma)^{41}\text{Sc}$  reaction in the range  $E_p = 1500$ – $3200$  keV. Three inserts show the yield of transitions to the first excited state. The resonances are labelled with the corresponding proton energies (in keV).

during the yield-curve measurements). For this purpose the yield curve is measured in several parts, each sandwiched between two measurements of the  $E_p = 1843$  keV resonance. The resonance strengths are deduced from areas of the resonance peaks, taking into account the branching ratios (see sect. 3.2). The determination of  $S$  from the yield curve for  $E_p > 2600$  keV is straightforward, since the detectors are positioned at  $\theta = +55^\circ$  and  $-55^\circ$ . A correction for the  $A_4$  coefficients reported by Youngblood *et al.*<sup>3)</sup> has been applied when they are not available from the present experiment (see table 3). For  $E_p < 2600$  keV the  $A_2$  term of the angular distribution has been estimated from the yields measured at  $\theta = 90^\circ$  and  $0^\circ$ , except for the  $E_p = 1621$  keV resonance where the  $A_2$  and  $A_4$  values reported in ref.<sup>3)</sup> are used as a standard.

During the yield-curve measurements a <sup>56</sup>Co  $\gamma$ -ray source was attached to the target. The <sup>41</sup>Sc  $\gamma$ -ray energies are determined relative to the energies of the <sup>56</sup>Co peaks<sup>19)</sup>. The excitation energies of the resonances with  $E_p < 2600$  keV listed in table 1, are deduced from the  $\theta = 90^\circ$  spectra. For the four resonances with  $E_p > 2600$  keV, the energies are calculated from the  $\theta = 55^\circ$  spectra. These resonances have total widths sufficiently large to ensure full Doppler shift:  $\Gamma(E_p = 2764 \text{ keV}) = 0.20 \pm 0.02 \text{ keV}$  [ref. <sup>1)</sup>], whereas the relations  $S = (2J + 1)\Gamma_p\Gamma_\gamma/\Gamma$  and  $\Gamma = \Gamma_p + \Gamma_\gamma$  lead to  $\Gamma > 4S/(2J + 1)$  for the other three resonances; the values of  $S$  are also given in table 1.

### 3.2. RESONANCE DECAY

The  $\gamma$ -ray decay has been measured of 21 <sup>41</sup>Sc levels with  $E_x < 4.5$  MeV. At each of the resonances a  $\theta = 55^\circ$  Compton-suppressed spectrum is recorded for about 12 h on-resonance and 6 h off-resonance. Most off-resonance spectra show a clear direct-capture transition to the first excited state, in agreement with the results of Terrasi *et al.*<sup>5)</sup>. The  $\gamma$ -ray decay of the weaker resonances at  $E_p = 647, 1363, 1977$ ,

TABLE 1  
Energies and strengths of <sup>40</sup>Ca(p,  $\gamma$ )<sup>41</sup>Sc resonances

$E_x$ (keV)		$E_p$ (keV) <sup>b)</sup>	$(2J + 1)\Gamma_p\Gamma_\gamma/\Gamma$ (meV)	
Present	Literature <sup>a)</sup>		Present	Literature <sup>c)</sup>
1716.44 $\pm$ 0.08	1718 $\pm$ 2	647.28 $\pm$ 0.05 <sup>d)</sup>		3
2095.9 $\pm$ 0.5	2096 $\pm$ 7	1036.3 $\pm$ 0.5		
2414.7 $\pm$ 0.5	2414 $\pm$ 5	1363.2 $\pm$ 0.5		
2588.06 $\pm$ 0.07	2588 $\pm$ 3	1540.87 $\pm$ 0.12	20 $\pm$ 3	17
2666.60 $\pm$ 0.07	2667 $\pm$ 3	1621.39 $\pm$ 0.12	18 $\pm$ 2	20
2719.12 $\pm$ 0.09	2717 $\pm$ 2	1675.24 $\pm$ 0.13	4 $\pm$ 1	
2882.43 $\pm$ 0.10	2882.8 $\pm$ 0.3	1842.66 $\pm$ 0.14	280 $\pm$ 30 <sup>e)</sup>	260 $\pm$ 40
2972.0 $\pm$ 0.2	2973 $\pm$ 3	1934.5 $\pm$ 0.2	62 $\pm$ 8	55
3013 $\pm$ 4		1977 $\pm$ 4		
3185.0 $\pm$ 0.2	3186 $\pm$ 3	2152.9 $\pm$ 0.2	200 $\pm$ 30	170
3411.4 $\pm$ 0.4	3416 $\pm$ 2	2385.0 $\pm$ 0.4	12 $\pm$ 4	6 $\pm$ 4 <sup>f)</sup>
3562.6 $\pm$ 0.3	3556 $\pm$ 20	2540.0 $\pm$ 0.3	23 $\pm$ 5	
3696.6 $\pm$ 0.3	3696.9 $\pm$ 0.5	2677.4 $\pm$ 0.3	300 $\pm$ 40	410
3780.6 $\pm$ 0.2	3783 $\pm$ 2	2763.5 $\pm$ 0.2	110 $\pm$ 15	150
4022.7 $\pm$ 0.4	4023 $\pm$ 3	3011.7 $\pm$ 0.4	77 $\pm$ 11	120
4030.1 $\pm$ 0.6	4031 $\pm$ 4	3019.3 $\pm$ 0.6	91 $\pm$ 14	130

<sup>a)</sup> Ref. <sup>1)</sup>.

<sup>b)</sup> Calculated from the present values of  $Q$  and  $E_x$ , unless indicated otherwise.

<sup>c)</sup> Calculated from  $S(r \rightarrow 0 \text{ MeV})$  reported in ref. <sup>1)</sup> and the present  $r \rightarrow 0$  MeV branching ratios, unless indicated otherwise.

<sup>d)</sup> See sect. 3.5.

<sup>e)</sup> Ref. <sup>9)</sup>.

<sup>f)</sup> Ref. <sup>6)</sup>.

2445, 2658 and 2755 keV that have not been observed in the present yield-curve measurements, could also be studied. In these cases the resonance energies are taken from literature <sup>1)</sup> or from the present work ( $E_p = 1977$  keV) and spectra are recorded at proton energies a few keV above and a few keV below the reported resonance energy  $E_p$ . The three resonances in the  $E_p = 3.2$ - $3.5$  MeV range of which the decay has been studied in detail (see below), could not be observed during the yield-curve measurement (fig. 1) due to machine instabilities.

The deduced branching ratios and upper limits are presented in table 2. Where a strong background line coincides with a potential primary no value can be given. All excited states of <sup>41</sup>Sc are proton unbound and in practically all cases one finds  $\Gamma_p \gg \Gamma_\gamma$ . As a consequence only one secondary transition has been detected in the present measurements. The ground-state decay from the  $E_x = 2.88$  MeV,  $E_p = 1843$  keV resonance has been observed not only at  $E_p = 1843$  keV, but also at the  $E_p = 2677$  and  $3242$  keV resonances which both decay to the  $E_x = 2.88$  MeV level. The ratios of the intensities of the primary and secondary transitions imply a ratio  $\Gamma_\gamma/\Gamma = 0.41 \pm 0.02$  for the  $E_x = 2.88$  MeV level, in good agreement with  $\Gamma_\gamma/\Gamma = 0.39 \pm 0.01$  reported by Kozub *et al.* <sup>4)</sup>. Combined with the known resonance strength  $S(1843 \text{ keV}) = 280 \pm 30 \text{ meV}$  and  $J(2.88 \text{ MeV}) = \frac{7}{2}$  this yields  $\Gamma_p = 85 \pm 10 \text{ meV}$ ,  $\Gamma_\gamma = 60 \pm 7 \text{ meV}$  and  $\Gamma = 145 \pm 15 \text{ meV}$ .

Upper limits for  $\Gamma_\gamma/\Gamma$  are determined from the measured spectra for the <sup>41</sup>Sc levels at  $E_x = 1.72, 2.10, 2.41, 2.59, 2.67, 3.01$  and  $3.19$  MeV as  $\Gamma_\gamma/\Gamma < 0.02, < 0.01, < 0.5, < 0.1, < 0.02, < 0.01$  and  $< 0.08$ , respectively.

### 3.3. THE $E_x = 3.01$ MeV LEVEL

A comparison of the level schemes of the mirror nuclei <sup>41</sup>Sc and <sup>41</sup>Ca is given in ref. <sup>1)</sup>. An excellent one-to-one relation is found up to  $E_x = 3.5$  MeV, with one exception. The counterpart of the  $E_x = 3.05$  MeV,  $J^\pi = \frac{3}{2}^-$  <sup>41</sup>Ca level is missing in the <sup>41</sup>Sc level scheme. From the  $\gamma$ -ray decay studies reported above (sect. 3.2), it is found that the  $E_p = 2764$  and  $3242$  keV resonances both decay to a previously not reported <sup>41</sup>Sc level at  $E_x = 3013 \pm 4$  keV, which would correspond to a proton energy of  $E_p = 1977 \pm 4$  keV. The  $\gamma$ -decay of the  $E_x = 3.01$  MeV level is measured in the same way as that of the other weak resonances (see sect. 3.2); the two observed branches are listed in table 2. Most probably this level is the counterpart of the <sup>40</sup>Ca level at  $E_x = 3.05$  MeV.

### 3.4. SPINS BASED ON TRANSITION STRENGTHS

The strength of a (p,  $\gamma$ ) resonance sets a lower limit to its total  $\gamma$ -ray width,  $\Gamma_\gamma > S/(2J+1)$ , and thus also to the strengths of all primary  $\gamma$ -ray transitions. Application of the recommended upper limits <sup>10)</sup> (RUL's) for  $\gamma$ -ray transition strengths then may result in the rejection of certain  $J^\pi$  values of the states involved.

TABLE 2  
Gamma-ray branchings (in %) of  $^{40}\text{Ca}(p, \gamma)^{41}\text{Sc}$  resonances <sup>a)</sup>

$E_p$ (keV)	$J_T^{\pi}$	$E_{\alpha}$ (MeV)	$E_{\alpha}^{\text{exc}}$ $J_T^{\pi}$	$1.72$ $\frac{1}{2}^-$	$2.10$ $\frac{1}{2}^+$	$2.41$ $\frac{3}{2}^-$	$2.59$ $\frac{3}{2}^-$	$2.67$ $\frac{3}{2}^+$	$2.72$ $\frac{1}{2}^+$	$2.88$ $\frac{1}{2}^+$	$3.01$ $(\frac{3}{2}^-, \frac{1}{2}^-)$
647	$\frac{1}{2}^-$	1.72	100								
1363	$\frac{1}{2}^-$	2.41	<5	100	<8						
1541	$\frac{1}{2}^-$	2.59	$97.6 \pm 0.3$	$2.4 \pm 0.3$	<0.3						
1621	$\frac{1}{2}^+$	2.67	$95.8 \pm 0.8$	$4.2 \pm 0.8$	<0.6						
1675	$\frac{1}{2}^+$	2.72	<7	100	<5						
1843	$\frac{3}{2}^+$	2.88	$99.92 \pm 0.03$	$0.08 \pm 0.03$							
1935	$\frac{1}{2}^-$	2.97	100	<0.2							
1977	$(\frac{1}{2}^-, \frac{3}{2}^-)$	3.01	$13 \pm 5$	$87 \pm 5$							
2153	$(\frac{3}{2}^-, \frac{9}{2}^+)$	3.19	100	<0.2	<0.2	<0.2	<0.2		<0.3		
2385	$\frac{1}{2}^+$	3.41	<2	100	<3	<3	<2	<3	<3	<3	
2445	$\frac{1}{2}^-$	3.47	<4	100							
2540	$(\frac{1}{2}^-, \frac{3}{2}^+)$	3.56	<13	100							
2658	$(\frac{3}{2}^-, \frac{1}{2}^-)$	3.68	$64 \pm 12$	$36 \pm 12$							
2677	$\frac{1}{2}^+$	3.70	$91.8 \pm 0.4$		$1.0 \pm 0.1$	<0.1	<0.1	$4.1 \pm 0.2$		$3.1 \pm 0.4$	<0.1
2755	$\frac{1}{2}^-$	3.77	100								
2764	$\frac{3}{2}^+$	3.78	$67 \pm 3$	$20 \pm 1$	$2 \pm 1$		$1 \pm 1$	$6 \pm 1$	$1 \pm 1$	$2 \pm 1$	$1 \pm 1$
3012	$\frac{1}{2}^-$	4.02	$71 \pm 1^b)$	$2.3 \pm 0.6$	$0.5 \pm 0.5$	<0.5	$2.0 \pm 0.5$	$24 \pm 1$	<0.5	<0.7	
3019	$\frac{1}{2}^-$	4.03	$98.0 \pm 0.6$	$2.0 \pm 0.6$	<0.2		<0.3			<0.4	
3242	$\frac{3}{2}^+$	4.25	$16.8 \pm 0.5$	$0.2 \pm 0.2$	$51 \pm 1$	$0.6 \pm 0.2$	$0.4 \pm 0.1$	$4.3 \pm 0.3$	<0.1	$11.7 \pm 0.6$	$15 \pm 1$
3325	$\frac{3}{2}^+$	4.33	$81.5 \pm 1.4$		<0.6	<0.9	$18.5 \pm 1.4$	<1	<0.7	$8 \pm 2$	
3440	$\frac{1}{2}^-$	4.44	$38.6 \pm 1.8^b)$		(and $21.0 \pm 1.5 \rightarrow 3.19$ MeV)		<0.7	$32.4 \pm 1.7$	<0.7		

<sup>a)</sup> Spins, excitation- and proton-energies are from the present experiment and from ref. <sup>1)</sup>.

<sup>b)</sup> Corrected for  $A_2$  coefficients of the angular distribution of the  $r \rightarrow 0$  MeV transition reported in ref. <sup>3)</sup>.

A  $J^\pi$  value is rejected if it implies a  $\gamma$ -ray transition strength exceeding the RUL by 1.5 standard deviation<sup>11)</sup>.

Along this line it is possible to determine the spin of the  $E_x = 2.41$  MeV level of <sup>41</sup>Sc. Previous (d, n) and ( $\tau$ , d) experiments result in the assignment<sup>1)</sup>  $J^\pi(2.41 \text{ MeV}) = (\frac{1}{2}, \frac{3}{2})^-$ . The present observation of a  $(0.6 \pm 0.2)\%$ ,  $E_x = 4.25 \rightarrow 2.41$  MeV branch combined with the known<sup>1)</sup> spin  $J^\pi(4.25 \text{ MeV}) = \frac{5}{2}^+$  and the resonance strength from table 1, would lead to an M2 strength of  $(35 \pm 12) \times 10^3$  W.u. for  $J^\pi(2.41 \text{ MeV}) = \frac{1}{2}^-$ . Since the M2 RUL is 3 W.u. one may conclude to  $J^\pi(2.41) = \frac{3}{2}^-$ .

The observed decay branches of the  $E_x = 3.01, 3.68, 3.70, 4.03$  and  $4.44$  MeV levels set limits to the possible spin values of the latter; see table 5.

### 3.5. THE REACTION Q-VALUE

In order to determine the <sup>40</sup>Ca(p,  $\gamma$ )<sup>41</sup>Sc reaction Q-value, precision  $E_\gamma$  and  $E_p$  measurements have been performed at the  $E_p = 647$  keV resonance. Two Ge(Li) detectors were positioned each at one side of the target at  $\theta = +90.0 \pm 0.5^\circ$  and  $\theta = -90.0 \pm 0.5^\circ$ . A <sup>56</sup>Co source was fixed to the target holder as close to the beam spot as possible. The resulting excitation energy is  $E_x = 1716.44 \pm 0.08$  keV.

The proton energy of this resonance is measured relative to that of the <sup>27</sup>Al(p,  $\gamma$ )<sup>28</sup>Si resonance at  $E_p = 654.65 \pm 0.04$  keV [ref. <sup>1)</sup>]. Thick-target yield curves of the two resonances are measured alternately at the same accelerator settings. A value of  $E_p = 647.28 \pm 0.05$  keV is obtained. With the known masses<sup>12)</sup> of the proton and of <sup>40</sup>Ca, this leads to a reaction Q-value of  $Q = 1085.07 \pm 0.09$  keV, to be compared with  $Q = 1085.5 \pm 1.0$  keV listed in ref. <sup>12)</sup>.

## 4. Angular distributions

### 4.1. MEASUREMENTS AND ANALYSIS

Gamma-ray angular distributions have been measured at the  $E_p = 2677, 3019$  and  $3242$  keV resonances. A moveable detector is placed at  $D = 4$  cm and at  $\theta = 0^\circ, 30^\circ, 45^\circ, 60^\circ$  and  $90^\circ$  and a monitor detector at  $D = 10$  cm and at a fixed backward angle. The angular sequence is measured repeatedly for about 10 min per angle during 10 to 15 h. The eccentricity of the set-up is measured at the  $E_p = 620$  keV, <sup>30</sup>Si(p,  $\gamma$ )<sup>31</sup>P resonance<sup>1)</sup>, which has  $J = \frac{1}{2}$  and thus an isotropic decay. The contents of the <sup>40</sup>Ca(p,  $\gamma$ )<sup>41</sup>Sc peaks in the spectra of the movable detector are normalised to the monitor yield and corrected for the measured eccentricity. A systematic error due to a possible shift of the target spot (at most 2 mm) between the <sup>30</sup>Si(p,  $\gamma$ )<sup>31</sup>P and the <sup>40</sup>Ca(p,  $\gamma$ )<sup>41</sup>Sc measurements is taken into account. The  $A_2$  and  $A_4$  coefficients listed in table 3 give a concise presentation of these data.

TABLE 3  
Angular distribution coefficients and mixing ratios

$E_p$ (keV)	$E_{x_i} \rightarrow E_{x_f}$ (MeV)	$J_i^\pi \rightarrow J_f^\pi$	$A_2$	$A_4$	$\delta$
2677	3.70 $\rightarrow$ 0	$\frac{7}{2}^+ \rightarrow \frac{7}{2}^-$	$0.44 \pm 0.04$	$-0.10 \pm 0.04$	$0.06 \pm 0.10$
	$\rightarrow$ 2.67	$\rightarrow \frac{5}{2}^+$	$-0.9 \pm 0.3$	$0.5 \pm 0.5$	$0.26 \pm 0.18$
3019	4.03 $\rightarrow$ 0	$\frac{7}{2}^- \rightarrow \frac{7}{2}^-$	$0.46 \pm 0.04$	$-0.27 \pm 0.04$	$-1.14 \pm 0.15$
3242	4.25 $\rightarrow$ 0	$\frac{5}{2}^+ \rightarrow \frac{7}{2}^-$	$-0.10 \pm 0.04$	$0.01 \pm 0.05$	$0.03 \pm 0.05$
	$\rightarrow$ 2.10	$\rightarrow \frac{3}{2}^+$	$-0.54 \pm 0.02$	$0.02 \pm 0.02$	$0.06 \pm 0.02$
	$\rightarrow$ 2.67	$\rightarrow \frac{5}{2}^+$	$0.36 \pm 0.07$	$-0.21 \pm 0.09$	$0.14 \pm 0.09^a)$

<sup>a)</sup> Or  $-1.8 \pm 0.3$ .

The deduced angular distributions are analysed as discussed in ref. <sup>7)</sup>. For the mixing ratios the sign convention of Rose and Brink <sup>13)</sup> is used.

## 4.2. RESULTS

**4.2.1. The  $E_p = 2677$  keV,  $E_x = 3.70$  MeV resonance level.** The transition strengths of the decay of the  $E_x = 3.70$  MeV level to the  $E_x = 2.67$  MeV,  $J^\pi = \frac{5}{2}^+$  and  $E_x = 0$  MeV,  $J^\pi = \frac{7}{2}^-$  levels only allow  $J^\pi(3.70 \text{ MeV}) = (\frac{3}{2}^- - \frac{9}{2}^+)$ . The angular distribution of the  $E_x = 3.70 \rightarrow 2.67$  MeV transition excludes the  $J^\pi = \frac{9}{2}$  and  $\frac{5}{2}^-$  solutions (see fig. 2a); the latter since the corresponding large  $\delta$  would imply an M2 strength of  $S > 1000 \pm 500$  W.u. The  $Q^2$  curves of the  $E_x = 3.70 \rightarrow 0$  MeV angular distribution, given in fig. 2b, reject the  $J^\pi(3.70 \text{ MeV}) = \frac{3}{2}^-$  and  $\frac{5}{2}^+$  solutions, since the corresponding large  $\delta$ 's lead to an M3 strength of  $S > (1.4 \pm 0.8) \times 10^6$  and an M2 strength of  $S > 110 \pm 50$  W.u., respectively, well above the M3 and M2 RUL's of 10 and 3 W.u., respectively. This leaves  $J^\pi(3.70 \text{ MeV}) = \frac{7}{2}$  as the only acceptable solution. A negative parity for this level can be rejected, since the  $(1.0 \pm 0.1)\%$  branch to the  $E_x = 2.10$  MeV,  $J^\pi = \frac{3}{2}^+$  level (see sect. 4.2.3.) would imply an M2 strength of  $S > 210 \pm 30$  W.u.

Conclusion:  $J^\pi(3.70 \text{ MeV}) = \frac{7}{2}^+$ .

**4.2.2. The  $E_p = 3019$  keV,  $E_x = 4.03$  MeV level.** The  $Q^2$  curves for the  $E_x = 4.03 \rightarrow 0$  MeV angular distribution are shown in fig. 2c. All solutions but  $J(4.03) = \frac{7}{2}$  can be rejected; the positive parity may be excluded because in that case the large mixing ratio  $\delta = -1.14 \pm 0.14$  would lead to an unacceptable M2 strength of  $S > 48 \pm 9$  W.u.

Conclusion:  $J^\pi(4.03 \text{ MeV}) = \frac{7}{2}^-$ .

**4.2.3. The  $E_x = 2.10$  MeV level.** Fig. 2d shows the  $Q^2$  curves for the  $E_x = 4.25 \rightarrow 2.01$  MeV angular distribution measured at  $E_p = 3242$  keV. Only two solutions are acceptable,  $J = \frac{3}{2}$  and  $\frac{7}{2}$ , of which  $J^\pi = \frac{7}{2}^-$  may be excluded on strength arguments. By combining the present result  $J^\pi = (\frac{3}{2}, \frac{7}{2}^+)$  with the  $J^\pi = (\frac{3}{2}, \frac{5}{2})^+$  assignment based on  $l_p = 2$  from ( $\tau, d$ ) experiments <sup>1)</sup>, one reaches the final conclusion  $J^\pi(2.10 \text{ MeV}) = \frac{3}{2}^+$ .

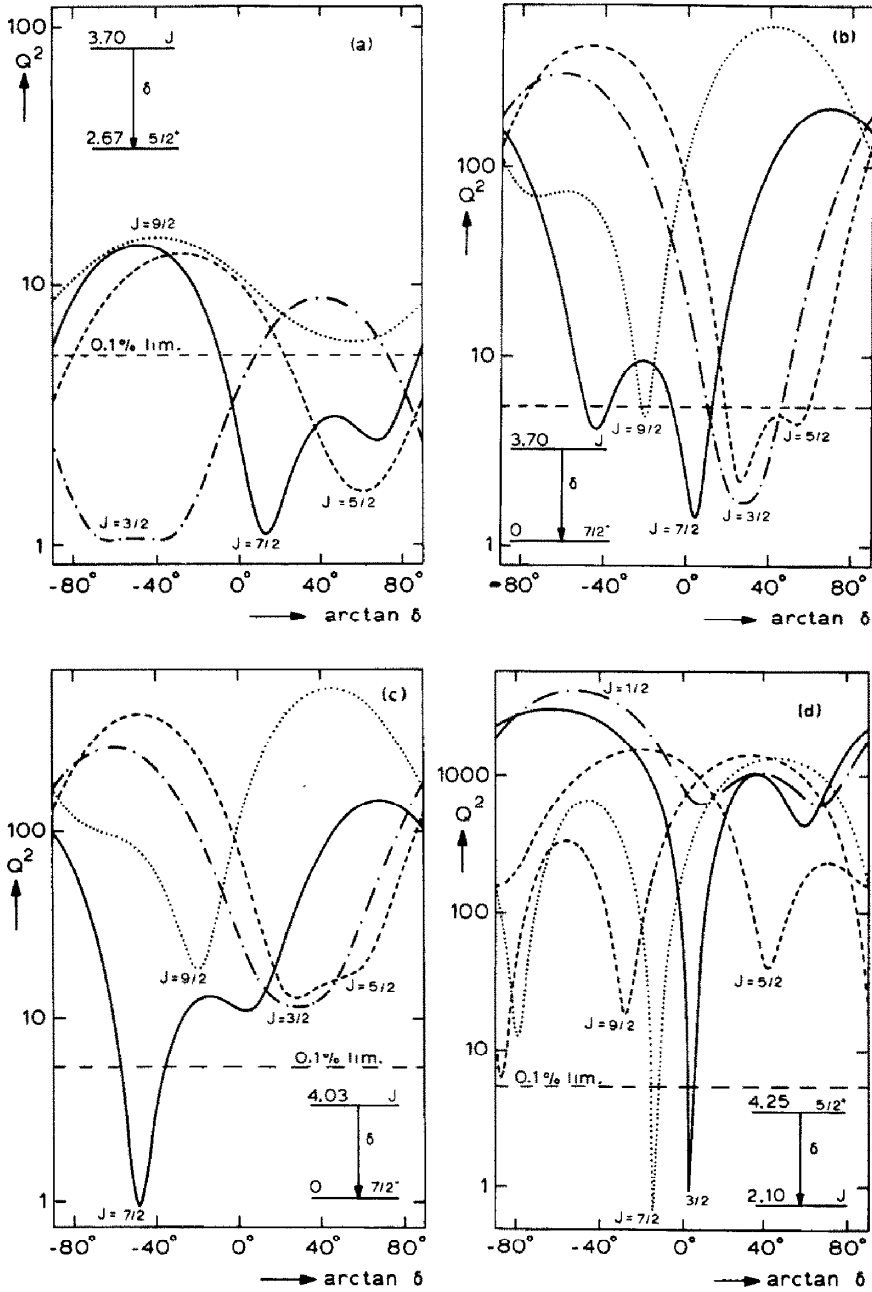


Fig. 2. Plots of  $Q^2$  versus  $\arctan \delta$  for the angular distributions of  $\gamma$ -ray transitions used to determine spins of <sup>41</sup>Sc levels. (a)  $E_p = 2677$  keV,  $E_x = 3.70$  MeV:  $r \rightarrow 2.67$  MeV. (b)  $E_p = 2677$  keV,  $E_x = 3.70$  MeV:  $r \rightarrow 0$  MeV. (c)  $E_p = 3019$  keV,  $E_x = 4.03$  MeV:  $r \rightarrow 0$  MeV. (d)  $E_p = 3242$  keV,  $E_x = 4.25$  MeV:  $r \rightarrow 2.10$  MeV.

### 5. Shell-model calculations

In order to give a shell-model description of the <sup>41</sup>Sc nucleus, calculations have been performed in the  $A = 38-42$  mass region, in a  $(2s_{1/2}1d_{3/2})^n(1f_{7/2}2p_{3/2})^m$  configuration space. The isospin formalism is used to describe states of the lowest two isospins: i.e.  $T = 0$  or  $1$  for even  $A$  and  $T = \frac{1}{2}$  or  $\frac{3}{2}$  for odd  $A$ . Excitations of at most three (four for  $A = 40$ ,  $T = 0$ ) particles from the sd shell to the fp shell are taken into account. States of both parities are described within the same model. The seniority  $\nu$  (the number of particles not coupled to spin zero) had to be limited to  $\nu \leq 4$  for three- and four-particle excitations.

The computer code RITSSCHIL<sup>16)</sup> is used for these calculations, which have been performed with the Cyber-205 computer of SARA, Amsterdam. The largest matrix dimensions which can reasonably be handled are about  $1000 \times 1000$ . The  $1d_{5/2}$ ,  $2p_{1/2}$  and  $1f_{5/2}$  sub-shells are therefore not considered in the model space; an inert core of <sup>28</sup>Si is thus assumed. This limitation is justified by the fact that the single-particle energies  $e(1d_{3/2} - 1d_{5/2}) \approx 6$  MeV,  $e(2p_{1/2} - 1f_{7/2}) \approx 4$  MeV and  $e(1f_{5/2} - 1f_{7/2}) \approx 6.5$  MeV [refs. <sup>14,15</sup>] suggest that excitations to or from these sub-shells may become significant only for levels at higher excitation energies.

The modified surface-delta interaction, used as the residual two-body interaction, is parametrized by three strength parameters:  $A_0$ ,  $A_1$  and  $B$  [ref. <sup>17</sup>]. In addition, three single-particle energies are used as parameters:  $e(1d_{3/2} - 2s_{1/2})$ ,  $e(1f_{7/2} - 2s_{1/2})$  and  $e(2p_{3/2} - 2s_{1/2})$ .

All states of the  $A = 38-42$  nuclides are described with this single set of only six parameters. Their values have been deduced empirically by fitting them to the excitation energies of all 120 known<sup>1)</sup> yrast and yrast + 1 levels of the low- $T$  nuclei in this mass range. No states have been excluded and all states have been given the same weight in the fitting procedure. The ensuring values of the strength parameters and the single-particle energies are (in MeV):

$$\begin{aligned} e(1d_{3/2} - 2s_{1/2}) &= 2.38, & A_0 &= 0.580, \\ e(1f_{7/2} - 2s_{1/2}) &= 4.02, & A_1 &= 0.449, \\ e(2p_{3/2} - 2s_{1/2}) &= 5.03, & B &= 0.504. \end{aligned}$$

The root-mean-square (RMS) deviation of the experimental and calculated excitation energies is about 500 keV for the 120 levels mentioned.

Nuclei from the sd shell as well as from the fp shell are described here with the same parameters. To examine the mass dependence of these parameters, fits have been performed for each mass number separately, as well as for the  $A = 38-39$  and  $A = 41-42$  systems. Only small deviations are found in the deduced parameters and level schemes. This supports the assumption that the interaction parameters can be considered constant in the mass region chosen here.

A detailed description of these calculations and the results (excitation energies, wave functions, transition strengths and spectroscopic factors) for the complete

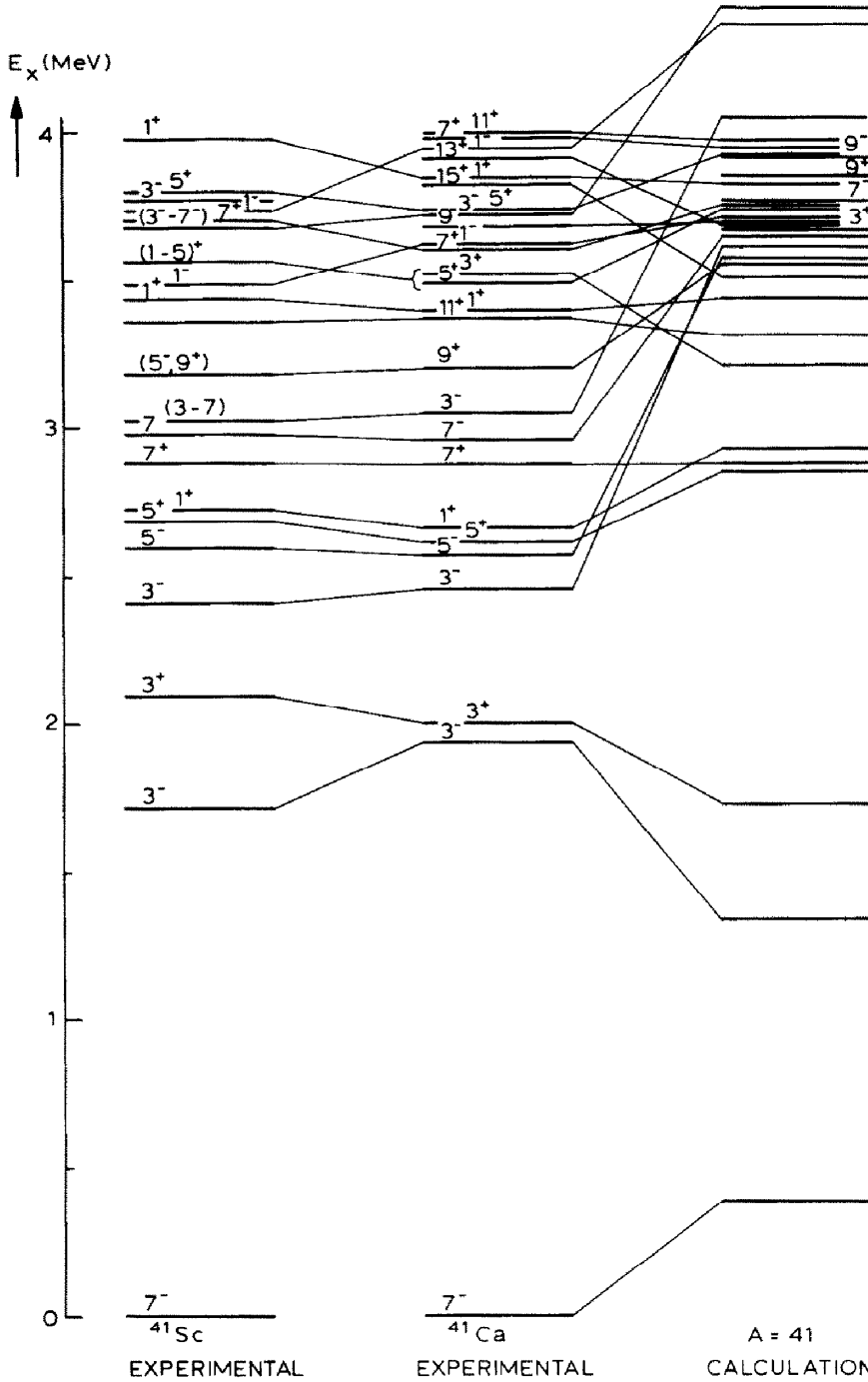


Fig. 3. Experimental level schemes of  $^{41}\text{Sc}$  and  $^{41}\text{Ca}$  and calculated level scheme of the  $T = \frac{1}{2}$  levels of  $A = 41$  nuclei. The levels are labelled with  $2J^\pi$ .

$A = 38-42$  mass region will be published in a forthcoming paper<sup>18</sup>). Here we only present the calculated excitation energies and transition strengths of the  $A = 41$ ,  $T = \frac{1}{2}$  system. Fig. 3 shows the experimental level schemes of <sup>41</sup>Sc and <sup>41</sup>Ca and the calculated  $A = 41$ ,  $T = \frac{1}{2}$  level scheme. All calculated and all experimentally known levels are drawn for energies below 4 MeV. Up to this energy a nearly one-to-one relationship exists both between the <sup>41</sup>Sc and <sup>41</sup>Ca levels and between the experimental and calculated levels.

The RMS deviation between the <sup>41</sup>Ca and the calculated  $A = 41$  level scheme is about 400 keV for  $E_x < 4$  MeV. The largest deviations occur for the  $J^\pi = \frac{3}{2}^-$  and  $\frac{5}{2}^-$  levels, which are calculated about 1 MeV too high. A possible influence of the  $2p_{1/2}$  and  $1f_{3/2}$  sub-shells, which are neglected in the present calculations, will be studied in the forthcoming paper mentioned above.

TABLE 4  
Measured and calculated transition strengths in <sup>41</sup>Sc

$E_{x_i} \rightarrow E_{x_f}$ (MeV)	$J_i^\pi \rightarrow J_f^\pi$ <sup>a)</sup>	Type	$S_x$ (exp.) <sup>b)</sup> (mW.u.)	$S_x$ (calc.) (mW.u.)
2.59 → 0	$\frac{5}{2}^- \rightarrow \frac{7}{2}^-$	M1	$8.8 \pm 1.3$	1.4
2.59 → 1.72	$\rightarrow \frac{3}{2}^-$	M1	$5.7 \pm 1.1$	0.014
2.97 → 0	$[\frac{7}{2}^-] \rightarrow \frac{7}{2}^-$	M1	$14 \pm 2$	17
3.70 → 2.67	$\frac{7}{2}^+ \rightarrow \frac{5}{2}^+$	M1	<140	370
3.70 → 2.88	$\rightarrow \frac{7}{2}^+$	M1	$100 \pm 20$	22
3.78 → 2.10	$\frac{5}{2}^+ \rightarrow \frac{3}{2}^+$	M1	$3.7 \pm 1.9$	230
3.78 → 2.67	$\rightarrow \frac{5}{2}^+$	M1	$38 \pm 8$	55
3.78 → 2.88	$\rightarrow \frac{7}{2}^+$	M1	$24 \pm 13$	310
4.02 → 0	$\frac{7}{2}^- \rightarrow \frac{7}{2}^-$	M1	$5.5 \pm 0.8$	11
4.02 → 2.59	$\rightarrow \frac{5}{2}^-$	M1	$3.4 \pm 1.0$	0.42
2.67 → 0	$\frac{5}{2}^+ \rightarrow \frac{7}{2}^-$	E1	$0.21 \pm 0.02$	0.30
2.67 → 1.72	$\rightarrow \frac{3}{2}^-$	E1	$0.20 \pm 0.04$	3.6
2.72 → 1.72	$\frac{1}{2}^+ \rightarrow \frac{3}{2}^-$	E1	$2.5 \pm 0.4$	64
2.88 → 0	$\frac{7}{2}^+ \rightarrow \frac{7}{2}^-$	E1	$3.1 \pm 0.4$ <sup>c)</sup>	14
3.19 → 0	$[\frac{9}{2}^+] \rightarrow \frac{7}{2}^-$	E1	$0.77 \pm 0.11$	13
3.42 → 1.72	$\frac{1}{2}^+ \rightarrow \frac{3}{2}^-$	E1	$1.5 \pm 0.5$	3.8
3.70 → 0	$\frac{7}{2}^+ \rightarrow \frac{7}{2}^-$	E1	$0.87 \pm 0.11$	26
3.78 → 0	$\frac{5}{2}^+ \rightarrow \frac{7}{2}^-$	E1	$0.28 \pm 0.04$	0.36
3.78 → 1.72	$\rightarrow \frac{3}{2}^-$	E1	$0.52 \pm 0.07$	0.07
4.02 → 2.67	$\frac{7}{2}^- \rightarrow \frac{5}{2}^+$	E1	$1.3 \pm 0.2$	1.0
1.72 → 0	$\frac{3}{2}^- \rightarrow \frac{7}{2}^-$	E2	$7200 \pm 1200$	7400
2.88 → 2.10	$\frac{5}{2}^+ \rightarrow \frac{3}{2}^+$	E2	$2900 \pm 900$ <sup>c)</sup>	4900
3.70 → 2.10	$\frac{7}{2}^+ \rightarrow \frac{5}{2}^+$	E2	$5300 \pm 900$	200
4.02 → 1.72	$\frac{7}{2}^- \rightarrow \frac{3}{2}^-$	E2	$540 \pm 160$	30

<sup>a)</sup> Square brackets indicate spins and parities from the corresponding <sup>41</sup>Ca levels.

<sup>b)</sup> Strengths are calculated from the resonance strengths assuming  $\Gamma_p \gg \Gamma_\gamma$ , and no radiation mixing, unless indicated otherwise.

<sup>c)</sup> Calculated from  $\Gamma_\gamma = 60 \pm 7$  meV deduced in the present experiment.

The calculated transition strengths are compared to the experimental data for <sup>41</sup>Sc in table 4. The transition strengths are grouped according to their transition type. Effective proton and neutron charges of 1.4*e* and 0.4*e*, respectively, are used in the calculation of the electric transition strengths, whereas bare *g*-factors are used for the magnetic transitions.

All calculated M1 transition rates in <sup>41</sup>Sc are small (much less than 1 W.u.) which is in agreement with experiment, see table 4. This can be understood, since these M1 transitions are largely *l*-forbidden, because their strengths are mainly determined by  $\Delta l = 2$ ,  $f \leftrightarrow p$  and  $s \leftrightarrow d$  single-particle transitions. Hence the measured M1 strengths strongly depend on small admixtures of e.g.  $1f_{5/2}$  and  $2p_{1/2}$  components. The latter admixtures are, however, not taken into account in the present calculations.

The theoretical E1 transition rates are highly sensitive to admixtures of spurious states in the wave functions. These admixtures cannot be removed in the present configuration space. The discrepancy between calculation and experiment shown in table 4 may probably largely result from this effect. Three of the measured E2 strengths shown in table 4 are not very small (larger than 1 W.u.). The calculation well reproduces the two fairly large transition rates between yrast states.

The discrepancies between calculation and experiment clearly show that – although the excitation energies are reproduced reasonably well – an adequate calculation of the small transition strengths requires a larger configuration space and possibly a more realistic interaction. Such an elaborate calculation, however, falls outside the scope of the present investigation.

## 6. Summary and discussion

This paper describes an experimental investigation of the <sup>41</sup>Sc levels with  $E_x < 4.5$  MeV via the reaction <sup>40</sup>Ca(*p*,  $\gamma$ )<sup>41</sup>Sc. Excitation and resonance energies have been deduced with high precision. Gamma-ray branching ratios are determined with a large-angle Compton-suppression spectrometer. Several transitions to excited states are established which have not been observed previously. Several resonances so far only observed in the reaction <sup>40</sup>Ca(*p*, *p*<sub>0</sub>)<sup>40</sup>Ca have been found also in the <sup>40</sup>Ca(*p*,  $\gamma$ )<sup>41</sup>Sc reaction. Angular distribution measurements lead to unambiguous spin assignments to four low-lying <sup>41</sup>Sc levels and to limitations for the possible spins of three more levels. Table 5 summarizes the spin and parity assignments.

This new information on spins, parities, branching- and mixing ratios in <sup>41</sup>Sc allows a detailed comparison with the mirror nucleus <sup>41</sup>Ca. The counterpart of <sup>41</sup>Ca(3.05 MeV) has been found in the present experiment. The counterpart of the  $E_x = 3.77$  MeV,  $J^\pi = \frac{3}{2}^-$  <sup>41</sup>Sc level, previously reported from (*p*, *p*<sub>0</sub>) experiments<sup>1)</sup>, has as yet not been found in <sup>41</sup>Ca. The existence of this <sup>41</sup>Sc level is confirmed in the present (*p*,  $\gamma$ ) experiment.

Shell-model calculations for  $A = 41$  are presented; the empirically deduced parameters are determined from all known low-*T* states in the  $A = 38$ –42 mass region.

TABLE 5  
Summary of spin and parity assignments

<sup>41</sup> Sc* (MeV)	Present experiment		Ref. <sup>1)</sup>	Conclusion
	decay	ang. distr.		
2.10		$\frac{3}{2}, \frac{7}{2}^+$	$(\frac{3}{2}, \frac{5}{2})^+$	$\frac{3}{2}^+$
2.41	$\frac{1}{2}^+ - \frac{9}{2}^+$		$(\frac{1}{2}, \frac{3}{2})^-$	$\frac{3}{2}^-$
3.01	$\frac{3}{2} - \frac{7}{2}$			$\frac{3}{2} - \frac{7}{2}$
3.68	$\frac{3}{2} - \frac{7}{2}$			$\frac{3}{2} - \frac{7}{2}$
3.70	$\frac{5}{2} - \frac{7}{2}^+$	$\frac{7}{2}$	$\frac{5}{2} - \frac{7}{2}$	$\frac{7}{2}^+$
4.03	$\frac{3}{2} - \frac{7}{2}$	$\frac{7}{2}^-$	$\frac{5}{2} - \frac{7}{2}$	$\frac{7}{2}^-$
4.44	$\frac{3}{2} - \frac{9}{2}^+$			$\frac{5}{2} - \frac{9}{2}^+$

Considering the fact that this mass region contains both sd and fp shell nuclei the results of these calculations are remarkably good. The calculated excitation energies of the lowest twenty <sup>41</sup>Sc levels are in acceptable agreement with the experimental data. The poor reproduction of most of the measured  $\gamma$ -ray transition strengths, however, indicates that more elaborate calculations are required.

The constructive criticism provided by Dr. C. Alderliesten and Prof. P.M. Endt was so thorough that we were not always able to appreciate it fully.

This work was performed as part of the research program of the "Stichting voor Fundamenteel Onderzoek der Materie" (FOM) with financial support from the "Nederlandse Organisatie voor Zuiver-Wetenschappelijk Onderzoek" (ZWO).

### References

- 1) P.M. Endt and C. van der Leun, Nucl. Phys. **A310** (1978) 1
- 2) E. Koltay, L. Mesko and L. Vegh, Nucl. Phys. **A249** (1975) 173
- 3) D.H. Youngblood, B.H. Wildenthal and C.M. Class, Phys. Rev. **169** (1968) 859
- 4) R.L. Kozub, B.E. Cooke, J.R. Leslie and B.C. Robertson, Phys. Rev. **C16** (1977) 132
- 5) F. Terrasi, A. Brondi, P. Cuzzocrea, R. Moro, G. La Rana, M. Romano, B. Gonsior, N. Notthoff and E. Kabuss, Nucl. Phys. **A394** (1983) 405
- 6) J.W. Maas, E. Somorjai, H.D. Graber, C.A. van den Wijngaart, C. van der Leun and P.M. Endt, Nucl. Phys. **A301** (1978) 213
- 7) F. Zijderhand, C.J. van der Poel, L.B. van Put and C. van der Leun, Nucl. Phys. **A451** (1986) 61
- 8) R.G. Sextro, R.A. Gough and J. Cerny, Nucl. Phys. **A234** (1974) 130
- 9) B.M. Paine and D.G. Sargood, Nucl. Phys. **A331** (1979) 389
- 10) P.M. Endt, At. Data and Nucl. Data Tables **23** (1979) 3
- 11) J.J.A. Smit, J.P.L. Reinecke, M.A. Meyer, D. Reitmann and P.M. Endt, Nucl. Phys. **A377** (1982) 15
- 12) A.H. Wapstra and G. Audi, Nucl. Phys. **A432** (1985) 1 and 55
- 13) H.J. Rose and D.M. Brink, Revs. Mod. Phys. **39** (1969) 306
- 14) W. Chung, thesis, Michigan State University (1976)
- 15) J.B. McGrory, Phys. Rev. **C8** (1973) 693
- 16) D. Zwarts, Comp. Phys. Comm. **38** (1985) 365
- 17) P.J. Brussaard and P.W.M. Glaudemans, in Shell-model applications in nuclear spectroscopy (North Holland, Amsterdam, 1977)
- 18) S.W. Kikstra, J.B.J.M. Lanen, F. Zijderhand and A.G.M. van Hees, (to be published)
- 19) R.G. Helmer, P.H.M. Van Assche and C. van der Leun, At. Data and Nucl. Data Tables **24** (1979) 39